

URANINITE: A 2 GA SPENT NUCLEAR FUEL FROM THE NATURAL FISSION REACTOR AT BANGOMBÉ IN GABON, WEST AFRICA

K.A. Jensen*, R.C. Ewing**, F. Gauthier-Lafaye***

*Department of Earth Sciences, Aarhus University, DK-8000 Aarhus C, keld@geo.aau.dk

**Department of Earth and Planetary Sciences, University of New Mexico, Albuquerque, NM 87131

***Centre National de la Recherche Scientifique, Centre de Geochemie de la Surface, 67084 Strasbourg Cedex, France

ABSTRACT

Uraninites from the Bangombé natural fission reactor (RZB) and “normal” uranium-ore occur as fine veins in the sandstone host-rock as well as altered, broken, and slightly displaced grains in an illitic matrix, and in nodules and veins of solid bitumen. Inclusions of galena, (Y,Gd)-rich phosphates, a Pb-oxide and a Ti-oxide? were observed. Uraninites just below RZB were partially altered to a uranyl-sulfate. Three generations of uraninite were identified based on their PbO-contents of 8-11.06 wt%, 6 wt% (the largest population), and a younger generation with 3 wt%. The high Pb-uraninites may be the precursor to the low Pb-uraninites. Diffusional loss of Pb is indicated by the presence of a Pb-oxide at the interface to the uraninites. The behaviour of the metallic fission products, incompatible with the uraninite structure, may mimic the behaviour of Pb in these uraninites. The averaged impurity-content ranges from 4.29 to 6.89 wt%, and consists mainly of SiO₂, TiO₂, ZrO₂, FeO, CaO, Al₂O₃ and P₂O₅. The averaged content of Y₂O₃ and the Ln's is less than 0.78 wt% and there is a scattered positive correlation with P₂O₅. The content of Y + Ln's is generally highest in the uraninites from RZB. Uraninite hydration and the formation of “uranopelite/zippeite” have caused complete loss of Y and the Ln's. These elements seems also to be partially lost by weak phosphatian coffinitization. The analytical results indicate that Y and the Ln's, which are high yield fission products, may be released from uraninite during alteration in the presence of P.

INTRODUCTION

Uraninite (UO_{2+x}) from the natural fission reactors and “normal” ore at Oklo, Okeleobondo and Bangombé in Gabon, West Africa, is studied as a natural analogue to the UO₂ in spent nuclear fuel [1,2,3,4,5]. A detailed study of the mineralogy of the Bangombé ore-deposit has recently been initiated. In this paper we present a preliminary petrographic and chemical description of uraninite from the Bangombé ore body. Our final goal is to obtain a better understanding of the long-term physical and chemical stability of uraninite in the geological environment.

The Bangombé uranium-ore deposit is located ~ 25 km W-NW of Franceville in SE-Gabon, and includes a high grade ore-body (~50 wt% U) in which natural fission reactions started approximately 1.97 Ga ago [1,2,6]. The ore body is situated in an anticlinal fold at the top of the FA-sandstone, the basal formation of the Lower Proterozoic sedimentary Franceville Series [1]. The amounts of fissiogenic Nd and Sm indicate that the maximum burnup of U-235 in RZB (Reactor Zone Bangombé) was approximately 1.25 %, and the neutron flux was up to 0.488 10²¹ n/cm² [6,7].

RZB has been verified in three drill-cores (BA145, BA145bis, and BAX03). In BAX03, the reactor core is approximately 5 cm thick (the maximum observed thickness in RZB) and located 11.80 to 11.85 m below the surface. This is approximately 1.1 m above the normal

water table in the drill hole [8]. In BAX03, the reactor core is overlain by a 0.3 m thick clay mantle which was produced by hydrothermal alteration of the surrounding rocks during criticality [2,9]. The clay mantle is covered by a 2.2 m thick layer of black shales (rich in organic material) followed by green pelites which both belong to the so-called FB-formation of the Franceville series [3,6]. In BA-145 and BA-145bis, RZB is very thin and located at 11.60 m depth. The uraninites in the RZB typically lie in an illitic groundmass. However, uraninite in the reactor samples from BA145 and BA145bis are also strongly associated with organic matter occurring as solid bitumen. Immediately beneath RZB, the FA-sandstone is highly silicified and contains nodules and veins of uraninite-bearing solid bitumen.

Since criticality ceased (after ~ 300,000 years of reactor operation [10]), the sediments in the Franceville basin have undergone a late diagenesis [11]. Subsequently, a 950-750 Ma regional thermal event associated with dolerite dyke emplacement caused local remobilization of U and a loss of Pb from most of the uraninites in the ore-bodies [5,12,13]. This resulted in abundant galena formation. At Oklo, a later remobilization event (330 Ma) has been suggested by Nagy et al. [14]. A similar age (375 Ma) was obtained by Gancarz [15], who argued that this was an artifact of volume diffusion of Pb. Today, the Bangombé uranium-deposit is exposed to supergene alteration. This involves kaolinitization of the phyllosilicates (illite and chlorite) and strong Fe-enrichment at about 9 m depth [6].

ANALYTICAL METHODS

The uraninite texture, alteration and mineral chemistry were studied in seven samples from four drill cores (BAX02, BAX03, BA-145 and BA-145ter; see Table 1). Sample 705 is from RZB; 854B and 859B are also from RZB or very close by. Sample 801 is from just below RZB in BAX03, while the samples 783, 786 and 790 are from BAX02 where criticality has not been demonstrated.

The textures were described by optical microscopy. The mineral chemistry was determined by electron microprobe analyses completed with a JEOL 733 Electron Microprobe at the University of New Mexico, and a JEOL JXA-8600 Superprobe at the Aarhus University, Denmark. The electron microprobes were operated with an acceleration voltage of 20 kV and a beam current of 20 nA. All elements were analysed with Wave Dispersion Spectrometry, except O, which was calculated by stoichiometry.

Table 1: Information about the samples used for the textural and chemical study of uraninite. Abbreviations: Ass. = associated, w/ = with, SB = solid bitumen.

Sample #	Drill-core	Depth (m)	Uraninite association
UNM783	BAX02	10.10-10.20	uraninite ass. w/ SB-nodules
UNM786	BAX02	11.45	uraninite ass. w/ SB-nodules and a thin uraninite vein
UNM790	BAX02	13.35	uraninite ass. w/ SB-nodules and a SB-vein
UNM801	BAX03	12.20-12.30	altered uraninite veins and grains in the sandstone
UNM705	BA145	11.00-11.80	uraninite grains in an illite matrix + in SB nodules
UNM854B	BA-145ter	11.60	uraninite ass. w/ SB-nodules and a SB-vein
UNM859B	BA-145	11.60	uraninite ass. w/ SB-nodules and in phyllosilicate veins

Nineteen elements (U, Th, Pb, Si, Ti, Zr, Ni, Co, Fe, Ca, Mg, Al, Sr, Y, La, Ce, Gd, and S) were analysed simultaneously with the JEOL 733. The standards included UO₂ (U); ThO₂ (Th); galena (Pb, S); kyanite (Si, Al); rutile (Ti); zirconia (Zr); metallic Ni and Co; chromite (Fe), scheelite (Ca); olivine (Mg); SrBaNb₄O₁₀ (Sr); and phosphates for P, Y, La, Ce and Gd.

The elements were analysed for a maximum of 40 sec or until 30,000 counts were reached on the peak position. The background positions were analysed for a maximum of 20 sec or until 15,000 counts. Results were accepted which had a standard deviation of 3 sigma or less on the counts. The JEOL 733 was operated with the Oxford Link system and data reduction was performed by ZAF-corrections.

On the JXA-8600, twenty elements were analysed in two sessions. Ni, Co and Sr from the setup on the JEOL-733 were not analysed. Instead, the content of Pr, Nd, Sm, and Eu were analysed in addition to the previously mentioned elements. The elements were calibrated against UO₂ (U); ThSiO₄ (Th); PbS (**Pb**); albite (Si, **Al**); CaTiO₃ (**Ca**, Ti); olivine (Mg); troilite (S), and phosphates for P, Y, La, Ce, Pr, Nd, Sm, Eu, and Gd. The underlined elements were analysed in the second session, while those in bold were analysed in both the first and second sessions to ensure a better matrix correction. The elements were analysed for up to 60 sec or until the standard deviation reached a value of 1%; the minimum time of measurement was, however, set to 5 sec. The background intensity was counted for 30 sec on each position. The results were accepted by exceeding the minimum detection limit. The JXA-8600 was operated with the Tracor Northern Software and data reduction was performed by PRZ-corrections.

Peak-overlaps between the Ln's (lanthanides), and between Nd_{Lα} and Pb_{Lα2} were controlled by measurements on the standards. The peak-overlaps between the Ln's are negligible at the measured concentrations. The Nd₂O₃-content was reduced by $[-(0.37/96) \cdot \text{wt}\% \text{PbO}]$.

RESULTS

In the "normal" uranium-ore outside RZB, the uraninites typically occur as up to 0.05 mm large inclusions in veins and nodules of solid bitumen (figure 1a). Uraninite outside RZB does, however, also appear in thin fracture veins and as single grains emplaced in quartz dissolution cavities in the sandstone close to the reactor (figure 1a and 2a,b).

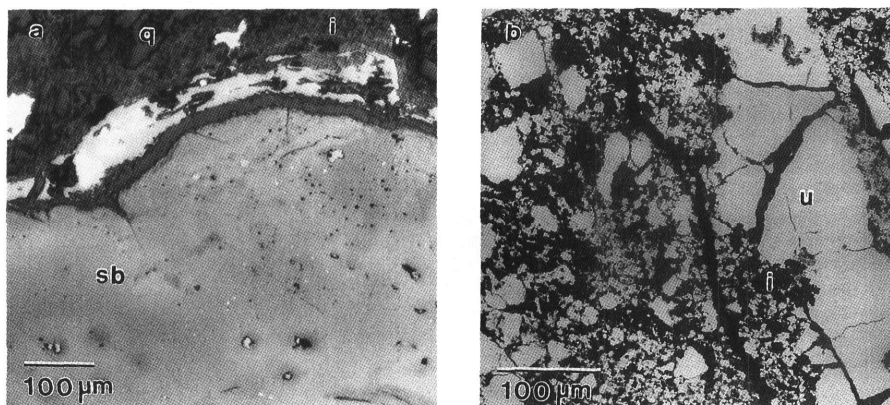


Figure 1: Microtextures observed in the samples from Bangombé U-ore body. **a)** Reflected light micrograph from 859B: Uraninite inclusions in a nodule of solid bitumen (sb) and a uraninite vein at the interface between the solid bitumen and the altered sandstone (q=quartz and i=illite). The grains with high reflectivity are galena. **b)** Backscattered electron image of 705 showing the corroded and brecciated uraninites (u) from the reactor core. The matrix mainly consists of illite (i).

In the reactor core (705), the uraninites lie in a groundmass of illite and minor amounts of Mg-rich chlorite partially impregnated with Fe_2O_3 (figure 1b). The grains are fractured and have a corroded rim. The grain size varies from a few microns to approximately 0.5 mm. Some of the fractured grains are slightly displaced. The uraninites in the other samples (854B and 859B) from or close to the reactor core mainly occur in association with solid bitumen. The sandstone in which these nodules and veins are emplaced is much more fractured as compared with the sandstone further from the RZB. These fractures are filled with uraninite, sulfides (galena, chalcopyrite and/or pyrite) and phyllosilicates. Uraninite also occurs as coatings on the solid bitumen.

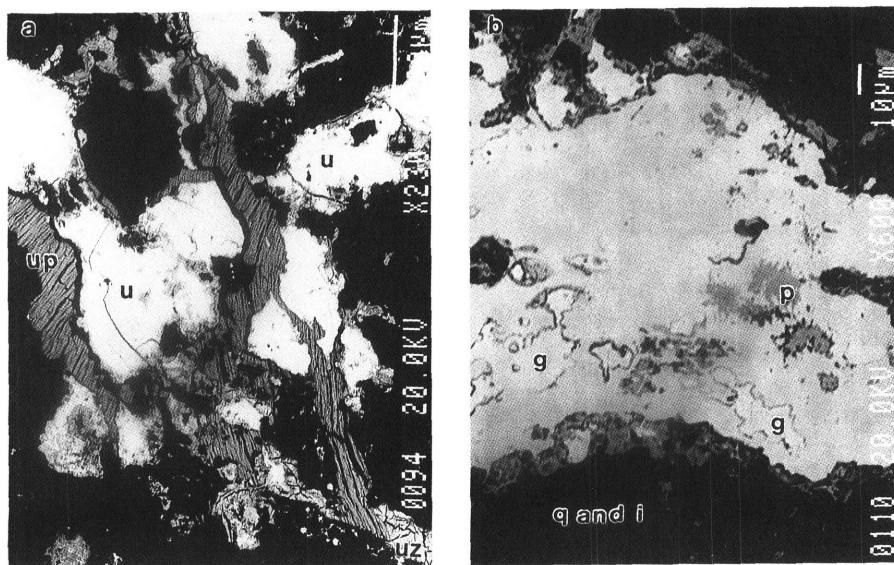


Figure 2: Backscattered electron images showing the microtextures observed in samples 801 (a) and 859B (b) from the Bangombé uranium ore-deposit. **a**) A vein filled with uranopelite/zippeite (uz) which has been cut by a later vein filled with a uranyl phosphate (up). Note the laminated structure of the uranyl phosphate. Uranopelite/zippeite also occurs at the rim of the corroded uraninites (u). The dark matrix consists of quartz. **b**) The image shows part of a uraninite vein in 859B. The uraninite vein contains inclusions of galena (g) and a Pb-oxide (minium Pb_3O_4) (p). The Pb-rich phase is also observed at the interface between the uraninite vein and the altered sandstone consisting of quartz (q) and illite (i).

The uraninites trapped in the solid bitumen often display a spherical anhedral morphology. Euhedral uraninites are seldom observed. The uraninite inclusions are sometimes broken and may be displaced by only a few tens of μm 's. The majority of the uraninite inclusions appear corroded, as observed in 705. The uraninite inclusions are also commonly rimmed by a TiO_2 -phase (rutile?). The solid bitumen generally appears as a compact and homogeneous solid. However, some of the solid bitumen veins have regions showing flow structures and regions where up to 0.25 mm large individual “drops” can be recognized.

Three samples (783, 801, 859B) from the FA-sandstone contain uraninite veins with a maximum thickness of approximately 0.5 mm. The uraninites in 801 have clearly been

subjected to hydrous alteration, as some of them are rimmed by a yellow-greenish alteration product. Microprobe analyses show the presence of U and S, and the phase may be either uranopelite $[(\text{UO}_2)_6\text{SO}_4(\text{OH})_{10}]\cdot 12(\text{H}_2\text{O})$ or zippeite $[(\text{UO}_2)_3(\text{SO}_4)_2(\text{OH})_2]\cdot 8(\text{H}_2\text{O})$. In 801 uranopelite/zip-peite was also observed in a vein which is cut by a later $\sim 75\text{ }\mu\text{m}$ wide fracture filled with a uranyl-phosphate (figure 2a). Recent alteration was observed in 790, where parts of a solid bitumen nodule, adjacent to an illite vein, contained UO_2 , but did not contain any Pb.

The uraninites normally contain small galena inclusions which are sometimes several μm large (figure 1a and 2b). Microprobe studies also indicate the presence of hydrous phosphate inclusions, rich in Y and Ln (see Y-phos; table 2). High Ti-contents in a few microprobe analyses indicate that Ti-oxide may also occur as inclusions in the uraninites. In 859B, several Pb-rich patches (minium: Pb_3O_4 ?) were observed in addition to abundant galena inclusions in a uraninite vein (figure 2b). The Pb-oxide was also observed at the interface to several of the uraninite veins in this sample.

A total of 113 sulfur free ($<0.05\text{ wt\%}$) uraninite compositions were analysed. The uraninites in 801 were very beam-sensitive, and the UO_2 -content decreased by almost 4 wt\% , when analysed as the last unknown. The same effect was observed for PbO. This may be due to partial hydroxylation of U. Representative analyses and average compositions for the uraninites are given in Table 2.

The uraninites primarily consist of UO_2 and PbO with up to almost 7 wt\% impurities (Table 2). The averaged UO_2 -content is quite constant and varies between 85.05 wt\% and 87.78 wt\% . The averaged PbO-content varies between 3.05 wt\% (801) and 7.74 wt\% (859B). However, some grains have higher PbO-contents (figure 3a). A plot of UO_2 vs. PbO shows that the analyses cluster around three compositions (figure 3a). One cluster is located at 88 wt\% UO_2 : 6 wt\% PbO and another at 87 wt\% UO_2 : 3 wt\% PbO . A third group contain 8 to 9 wt\% PbO , and a single grain has a PbO-content of 11.06 wt\% .

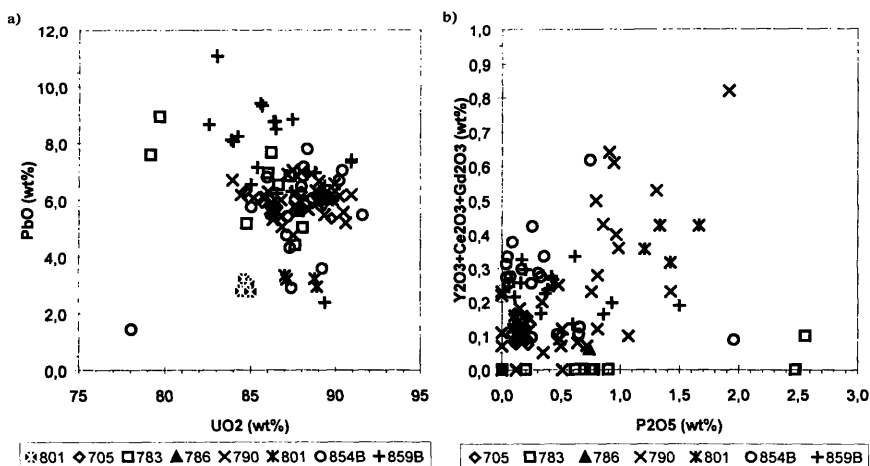


Figure 3: a) Plot of the UO_2 vs. PbO in the unaltered uraninites (Table 1) from the Bangombé U-ore body. b) Plot of P_2O_5 vs. $\text{Y}_2\text{O}_3+\text{Ce}_2\text{O}_3+\text{Gd}_2\text{O}_3$ for all the unaltered uraninites.

Table 2: Uraninite analyses in wt.% from the U-ore deposit at Bangombé. The last two analyses are a phosphate inclusion (Y-phos) in a uraninite grain and a completely hydroxylized uraninite grain (UranOH). Sample number 705 is from RZB. 854B and 859B are also from RZB or very close by. The other samples represent the “normal” U-ore body. Abbreviations: n is number of grains analysed. - not analysed element. < the average content (if present) and the standard deviation for the population (shown in brackets) is below 0.01.

Oxide	783 (n=9)	786 (n=1)	790 (n=31)	801 (n=9)	854B (n=19)	859B (n=21)	705 (n=23)	783 Y-phos	786 UranOH
UO ₂	85.05 (3.15)	87.78	85.19 (1.73)	86.16 (1.73)	87.04 (2.70)	86.29 (2.44)	87.36 (1.72)	58.94	77.16
ThO ₂	<	<	<	0.12 (0.03)	0.01 (0.02)	<	0.09 (0.03)	<	<
SiO ₂	0.94 (0.65)	0.40	0.89 (0.21)	0.14 (0.06)	0.83 (0.28)	0.80 (0.27)	0.98 (0.18)	5.31	0.27
TiO ₂	2.23 (1.46)	0.86	1.26 (0.70)	0.36 (0.13)	2.32 (2.11)	0.79 (0.65)	0.25 (0.07)	1.21	<
ZrO ₂	<	0.14	0.06 (0.10)	0.16 (0.06)	1.01 (0.49)	0.08 (0.05)	0.28 (0.22)	<	<
PbO	6.59 (1.38)	5.63	5.85 (0.59)	3.05 (0.20)	5.41 (1.58)	7.74 (1.67)	5.99 (0.31)	0.86	<
SnO	<	<	0.03 (0.04)	-	-	-	-	<	<
NiO	0.01 (0.01)	0.03	0.03 (0.02)	-	-	-	-	<	<
CoO	<	<	0.01 (0.02)	-	-	-	-	<	<
FeO	0.77 (0.16)	0.44	0.58 (0.26)	1.11 (0.10)	0.63 (0.09)	0.81 (0.30)	0.62 (0.11)	0.12	0.07
CaO	0.52 (0.36)	1.62	1.46 (0.37)	0.49 (0.13)	1.12 (0.37)	1.07 (0.36)	1.11 (0.13)	1.71	<
MgO	0.02 (0.01)	0.02	0.08 (0.05)	0.04 (0.01)	0.03 (0.01)	0.03 (0.01)	0.38 (0.10)	<	<
Al ₂ O ₃	0.47 (0.42)	0.19	0.22 (0.13)	0.27 (0.04)	0.11 (0.07)	0.08 (0.03)	0.12 (0.05)	0.65	0.01
P ₂ O ₅	1.00 (0.86)	0.74	0.60 (0.47)	1.38 (0.12)	0.39 (0.43)	0.41 (0.34)	0.18 (0.05)	8.95	<
Y ₂ O ₃	<	<	0.11 (0.18)	0.01 (0.01)	0.07 (0.05)	0.03 (0.03)	0.01 (0.02)	2.61	<
La ₂ O ₃	-	-	-	0.07 (0.02)	0.02 (0.02)	0.02 (0.02)	0.02 (0.02)	-	-
Ce ₂ O ₃	0.01 (0.03)	0.06	0.12 (0.08)	0.30 (0.03)	0.17 (0.06)	0.16 (0.04)	0.09 (0.02)	0.09	<
Pr ₂ O ₃	-	-	-	0.05 (0.04)	0.01 (0.03)	0.01 (0.01)	0.01 (0.02)	-	-
Nd ₂ O ₃	-	-	-	0.27 (0.04)	0.09 (0.05)	0.12 (0.05)	0.09 (0.03)	-	-
Sm ₂ O ₃	-	-	-	0.04 (0.02)	0.02 (0.03)	0.05 (0.04)	0.02 (0.03)	-	-
Eu ₂ O ₃	-	-	-	<	<	<	<	-	-
Gd ₂ O ₃	<	<	<	0.04 (0.03)	0.05 (0.09)	0.03 (0.03)	0.01 (0.02)	0.76	<
S	0.01 (0.02)	<	< (0.01)	<	0.01 (0.01)	0.01 (0.01)	0.04 (0.02)	<	<
Total	97.62 (1.55)	97.91	96.49 (2.00)	94.06 (2.03)	99.34 (1.71)	98.52 (1.97)	97.64 (1.79)	81.21	77.51

The impurities (all elements other than UO_2 and PbO) mainly consist of SiO_2 , TiO_2 , ZrO_2 , FeO , CaO , Al_2O_3 and P_2O_5 , and the averaged content varies between 4.29 wt% (705) and 6.89 wt% (854B). The average content of TiO_2 and CaO (less than 2.32 and 1.62 wt% respectively) is typically higher than the SiO_2 -content. The SiO_2 -content is usually below 1 wt% and shows that penetrative coffinitization ($\text{UO}_2 \rightarrow \text{U}[\text{SiO}_4] \cdot n\text{H}_2\text{O}$) is very limited. The composition of the impurities in 801 are significantly different from the other samples: the contents of SiO_2 and CaO is lower, whereas P_2O_5 , TiO_2 , FeO , ThO_2 , Ce_2O_3 and Nd_2O_3 are higher (Table 2).

The concentration of $\text{Y}_2\text{O}_3 + \text{Ln}$'s is normally less than 1 wt%. The maximum averaged concentration of these oxides is observed in 801 (0.78 wt%, Table 2). The analyses show that Ce_2O_3 and Nd_2O_3 are the most abundant Ln's. Eu_2O_3 occurs with very low concentrations; the mean value is always close to zero. A scattered positive correlation is observed between P_2O_5 and $\text{Y}_2\text{O}_3 + \text{Ce}_2\text{O}_3 + \text{Gd}_2\text{O}_3$ (figure 3b). The overall correlation is slightly obscured by differences in the REE-content between the various samples. This is especially notable for the uraninites in 854B and 859B, which have relatively high $(\text{Y}_2\text{O}_3 + \text{Ce}_2\text{O}_3 + \text{Gd}_2\text{O}_3)/\text{P}_2\text{O}_5$ -ratios.

Homogeneity and extent of alteration of the uraninites were examined in the samples 705, 801 and 859B. The results show that the uraninites are quite homogeneous in 705 and 801, although they sometimes have abrupt compositional variations. The grains are sometimes zoned in their content of Y-, Ce and Nd-oxides and have maximum concentrations in the interior. Figure 4 shows the variation of selected elements across a partially coffinitized uraninite vein in 859B. The linescan shows an increase in SiO_2 , TiO_2 , FeO , CaO , and P_2O_5 at the rim of the vein associated with a strong decrease in PbO , and minor decrease of Ce_2O_3 , and Nd_2O_3 . The central area in the scan has an increased content of UO_2 (~ 3.2 wt%), P_2O_5 (~ 0.6 wt%) and SiO_2 (~ 0.2 wt%), and a small decrease in Ti- and Ce-concentration; ~ 0.1 and ~ 0.02 oxide wt%, respectively. The results indicate that the partial coffinitization has resulted in a loss of Pb and a weak loss of the Ln's.

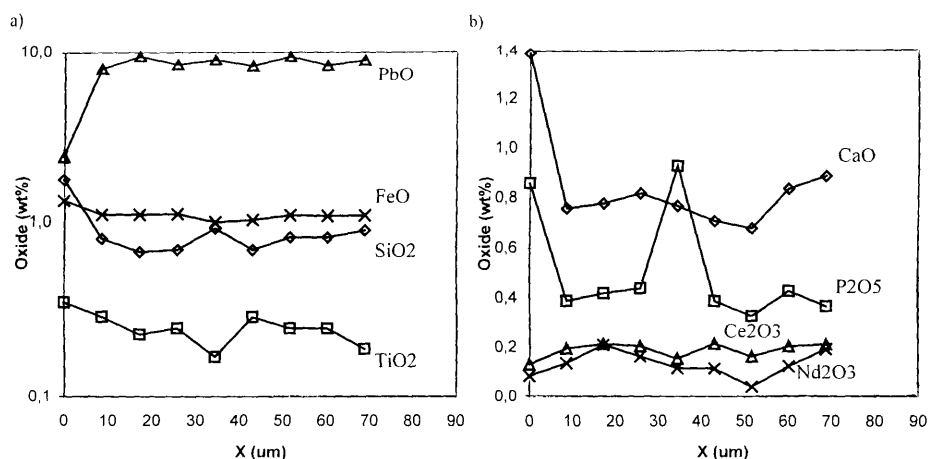


Figure 4a,b: Results from a linescan showing selected oxide contents from the edge of a vein (left) in 859B to an area with galena inclusions. Note that the abscissa in (a) is logarithmic.

DISCUSSION

The general textural features of the uraninites observed are consistent with previous observations [3,16,17]. However, some of the new observations are the presence of the phosphate inclusions, the Pb-oxide associated with the uraninite veins just below RZB, the uranyl phases, and the locally hydrous altered uraninites in the sandstone close to RZB.

The morphology of the individual uraninite grains in the ore-body suggests that most of the grains have been subjected to corrosion at some time during their geological history. However, the homogeneity of the uraninites in 705 indicates that this ancient corrosion had negligible effect on the present day chemistry of the residual grains. The presence of corroded uraninite inclusions and broken grains in the solid bitumen suggest that either (1) corrosion of these uraninites occurred before they were trapped by the organic matter, and/or (2) the solid bitumen no longer protects the uraninites against hydrous alteration at Bangombé. This needs to be further clarified.

The chemistry of the uraninites is complex and they contain a wide variety of impurities which add up to 7 oxide wt% in addition to the PbO-content. Based on ionic radii, the majority of the most abundant impurities (Si, Ti, Zr, Pb, Al, and P) are not expected to substitute for U in uraninite. However, experimental studies have shown that approximately 0.2 wt% ZrO₂ can substitute for synthetic UO₂ at 1473°K and the amount increases at higher temperatures ($T > 1573^\circ\text{K}$) [18]. Only the ZrO₂-content in the uraninites in sample 705 from RZB, which formed at much lower temperatures, exceed this experimental value (table 2).

The PbO-content in the uraninites indicates the presence of three generations of uraninite: (1) The high PbO-generation (8-11 wt% PbO); (2) the 6 wt% PbO generation, which has been observed before [5]; and (3) the 3 wt% PbO generation, which was observed in fracture veins and nodules of solid bitumen with flow structures. The events related to generations 2 and 3 are presently unknown, but texturally generation 3 seems to have been formed by remobilisation of U and organic matter. This is further supported by the distinct difference in the composition of the minor elements as compared with the other grains (higher contents of Th, Y and Ln's are most significant). The high Pb-uraninites in generation 1 have similar PbO-contents (~10 wt%) as those which recrystallized during the regional heating 950-750 Ma ago (see [5]). At least the uraninites with intermediate PbO-contents may have been produced by diffusional loss of Pb from the high Pb-uraninites. This is further indicated by the presence of the Pb-oxide which occurs in association with the uraninite veins in 859B (figure 2b).

Lead is not of concern with respect to the disposal of spent nuclear fuel. However, this behaviour of Pb in uraninite may resemble the behaviour of the metallic fission products (e.g. Mo, Tc, Ru, Rh, and Pd) in spent nuclear fuel, as previously suggested by Janeczek and Ewing [5]. In that respect, figure 2b then becomes quite important since it shows that such elements may be liberated from the UO₂-matrix to the surrounding environment where the distance of migration will depend on the local physico-chemical conditions.

Yttrium and the Ln's are among the high yield fission products of U-235 and are expected to appear in high concentrations in the samples from the RZB (705, 859, and 854B). Experimental studies have shown that these elements are easily incorporated into synthetic UO₂ with more than 48 mole% at temperatures above 1273°K [18]. Phosphorus may also be produced during fission reactions by neutron capture by Si. A positive correlation between P and Y+Ln is then expected as shown in figure 3, but the (Y₂O₃+Ce₂O₃+Gd₂O₃)/P₂O₅-ratio shows that P is more dominant in the uraninites from outside RZB. This suggests that the primary ore-forming fluids had a relatively high concentration of P rather than P having been formed during the fission reactions. The heat released during the fission reactions and/or the

regional heating 950-750 Ma ago may have caused aggregation of the impurities and formation of the phosphate inclusions. Apatite inclusions with fissionogenic Ln have been reported from reactor zone 10 at Oklo [19]. The hydrothermal influence during the fission reactions, diagenesis and subsequent regional heating may have caused additional loss of P from RZB. This release of P and combination with actinides and Ln's could explain the formation of crandallite group minerals with fissionogenic Ln's which are observed in the surrounding rocks at Bangombé [7].

Coffinitization has previously been described as a mechanism for the alteration of uraninite under reducing conditions [e.g. 20]. Even though coffinite is a well known alteration product, the elemental behaviour of the impurities in uraninite during coffinitization is almost unknown. This investigation and previous studies [20] indicate that Pb is readily lost from uraninite by this process. However, loss of Pb may also be caused by diffusion, as the low Pb-content is observed in the outer 10 μm of the vein (figure 3). The behaviour of Y and the Ln's is unclear at this stage of alteration. However, the Ce and Nd contents seem to decrease at the rim of the vein. Loss of Y and Ln's during coffinitization is unexpected, but similar behaviour was observed in reactor zone 10 at Oklo [21].

Hydrous alteration results in the formation of uranyl phases such as schoepite, uranopelite, zippeite and uranyl orthophosphate. The hydrous alteration phases observed here are possibly uranopelite or zippeite and hydroxylized uraninite/schoepite (Table 2). Microprobe studies of these grains indicated no presence of Y and Ln. Hence these elements do not appear to substitute for U in the uranyl phases and therefore seem to be lost during the hydrous alteration.

CONCLUSIONS

- The uraninites from the Bangombé ore deposit are generally corroded and partially altered. They occur in an illite matrix (RZB), as veins and grains in the sandstone, and as inclusions in veins and nodules of solid bitumen. The uraninites contain inclusions of Y- and Ln-rich phosphates, a Ti-oxide, a Pb-oxide, and galena.
- Three generations of uraninites with 8 to 11.06 wt%, 6 wt%, and 3 wt% PbO are observed.
- The impurities in the uraninites mainly consist of SiO_2 , TiO_2 , ZrO_2 , FeO, CaO, Al_2O_3 and P_2O_5 and reach a maximum average concentration of 6.89 wt%, in addition to the content of PbO. The average content of Y_2O_3 and the Ln's is less than or equal to 0.78 wt%.
- Loss of Pb seems to have occurred by diffusion from some uraninites and resulted in the formation of a Pb-oxide at the rim of the vein in sample 859B. The behaviour of metallic fission products in spent nuclear fuel may resemble the behaviour of Pb in these uraninites.
- The uraninites from or close to RZB have a higher content of Y and Ln's relative to P as compared with the normal uranium ore. Y+Ln has a positive correlation with P. Hence, P may have been an important constituent of the primary ore-forming fluids. Phosphorus may also have played a role in actinide and REE-migration from the RZB.
- Coffinitization is very limited, but this process is related to Pb-release from the uraninites and may also be related to the release of Y and Ln's in the presence of P.
- The uraninites have locally been subjected to hydrous alteration. In some cases this has resulted in the formation of uranyl phases and loss of Y and the Ln's.

ACKNOWLEDGEMENTS

We thank the Commissariat à l'Énergie Atomique, France, for providing the well-documented samples; Janusz Janeczek for discussions of the analytical results; and Sidsel Grundvig and

Mike Spilde for their assistance during the microprobe sessions. The work was supported by the Faculty of Science, Aarhus University, Denmark and the *Svensk Kärnbränslehantering AB* (SKB), Stockholm, Sweden. The work was performed in cooperation with the Oklo Working Group organized by the European Union and the Commissariat à l'Energie Atomique, France. The electron microprobe in the Department of Earth and Planetary Sciences, University of New Mexico was supported by NSF, NASA, DOE/BES, and the State of New Mexico. The electron microprobe at the Department of Earth Sciences, Aarhus University was supported by *Statens Naturvidenskabelige Forskningsråd*, *Carlsbergfondet*, and *Aarhus Universitetsfond*.

REFERENCES

- [1] F. Gauthier-Lafaye and F. Weber, *Econ. Geol.*, **84**, 2267-2285 (1989)
- [2] F. Gauthier-Lafaye, F. Weber, and H. Ohmoto, *Econ. Geol.*, **84**, 2286-2295 (1989)
- [3] F. Gauthier-Lafaye, Rapport final; Volume 2: Les Reacteurs de Fission et les Systemes Geochemiques; 2ème partie: Geologie des reacteurs, études des épontes et transferts anciens, Commissariat à l'Energie Atomique. Institution de Protection et de Sûreté Nucléaire, 105-118 (1995).
- [4] P.-L., Blanc, Final report: Volume 1: Acquierements of the natural analogy programme. Commissariat à l'Energie Atomique, Institut de Protection et de Sûreté Nucléaire, 135 pp. (1995)
- [5] J. Janeczek and R.C. Ewing, *Geochim. Cosmochim. Acta*, **59**, 1917-1931 (1995)
- [6] R. Bros, F. Gauthier-Lafaye, P. Larque, and P. Stille, Mineralogy and isotope geochemistry of Bangombé reaction zone - Migrations of U, Th and fission products. Internal report for SKB-CNRS "Oklo - Analogues Naturels", Centre National e la Recherche Scientifique, Centre de Geochemie de la Surface, 1, rue Blessig, 67084 Strasbourg Cedex, France, 14 p. (1993)
- [7] J. Janeczek and R.C. Ewing, *Am. Min.*, **81**, 1263-1269 (1996)
- [8] P. Toulhaut, J.P. Gallien, D. Louvat, V. Moulin, P. l'Henoret, R. Guerin, E. Ledoux, I. Gurban, J.A.T. Smellie, and A. Winberg, Fourth International Conference on the Chemistry and Migration Behaviour of Actinides and Fission Products in the Geosphere. Charleston, SC USA, December 12-17, 1993), 383-390.
- [9] P.O. Eberly, R.C. Ewing, J. Janeczek, and A. Furlano, *Radiochim. Acta*, **74**, 271-275 (1996).
- [10] Ph. Holliger, Terme Source: Caracterisation Isotopique Parametres Nucleaires et Modelisation. Commissariat à l'Energie Atomique, Institut de Protection et de Sûreté Nucléaire, p. 40 (1994)
- [11] M.G. Bonhomme, F. Gauthier-Lafaye, and F. Weber, *Precambrian Research*, **18**, 87-102 (1982)
- [12] F. Gauthier-Lafaye, P. Holliger, and P.-L. Blanc, *Geochim. Cosmochim. Acta*, in press (1996)
- [13] P.O. Eberly, J. Janeczek, and R.C. Ewing, *Radiochim. Acta*, **66/67**, 455-461 (1994)
- [14] B. Nagy, F. Gauthier-Lafaye, Ph. Holliger, D.W. Davis, D.J. Mossman, J.S. Leventhal, M.J. Rigali, and J. Parnell, *Nature*, **354**, 472-475 (1991)
- [15] A.J. Gancarz, Natural Fission Reactors, (Proc. Tech. Comm. Meet., Paris, December 1977, International Atomic Energy Agency: Vienna), 513-520 (1978)
- [16] J. Janeczek, and R.C. Ewing, In Nuclear Science and Technology - Report EUR 16098 edited by H. von Marevic (Oklo Working Group - Proceedings of the third joint EC-CEA progress meeting held in Brussels on 11 and 12 October 1993, 181-211 (1995)
- [17] B. Nagy, In Nuclear Science and Technology - Report EUR 16098 edited by H. von Marevic (Oklo Working Group - Proceedings of the third joint EC-CEA progress meeting held in Brussels on 11 and 12 October 1993, 169-179 (1995).
- [18] H. Kleykamp, *J. of Nucl. Mat.*, **206**, 82-86 (1993)
- [19] H. Hidaka, K. Takahashi, and Ph. Holliger, *Radiochim. Acta*, **66/67**, 463-468 (1994).
- [20] J. Janeczek, and R.C. Ewing, *J. Nucl. Mat.*, **190**, p. 157 (1992).
- [21] R.C. Ewing and J. Janeczek, In Nuclear Science and Technology - Report EUR 14877EN edited by H. von Marevic (Oklo Working Group - Proceedings of the second joint CEC-CEA progress meeting held in Brussels on 6 and 7 April 1992, 177-188 (1993).